Marine and Petroleum Geology 139 (2022) 105636

Contents lists available at ScienceDirect

Marine and Petroleum Geology

journal homepage: www.elsevier.com/locate/marpetgeo

A case study in controlled source electromagnetism: Near seabed hydrocarbon seep systems of Coal Oil Point, California, USA

Roslynn B. King [a,b,*], Steven Constable [a], Jillian M. Maloney [b]

[a] Scripps Institution of Oceanography, University of California San Diego, La Jolla, CA, 92093, USA
[b] Department of Geological Sciences, San Diego State University, 5500 Campanile Dr., San Diego, CA, 92182-1020, USA

ARTICLE INFO

Keywords:
CSEM
Marine hydrocarbon seeps
Seep geology

ABSTRACT

Marine hydrocarbon seeps are found on all continental margins and release significant amounts of greenhouse gases and hydrocarbons into the atmosphere and hydrosphere. Most methods of studying seeps rely on seafloor or near-seafloor observations, but seepage rates and seep locations can be variable, leading to uncertainty. We exploit the fact that hydrocarbons are electrically resistive compared with surrounding sediments and use marine electromagnetic methods to study the deeper sources and accumulation sites, which are controlled by local geology and should be more stable than the seabed expressions. Our surface towed marine controlled source electromagnetic system used a horizontal electric dipole transmitter and floating electric dipole receivers spaced 100–400 m from the transmitter, collecting frequency domain amplitude and phase data at ~2 Hz and harmonics. The survey targeted known and inferred hydrocarbon seeps within the Coal Oil Point seep field offshore Santa Barbara, California, USA. Two dimensional inversions of the data indicate that the method is sensitive to the shallowly buried (<400 m) structure of the marine hydrocarbon seeps and is an efficient and effective tool in their identification and characterization. The results show spatial variability of seafloor hydrocarbons along the Coal Oil Point seep field and indicate at least two previously unidentified intermediate depth accumulation sites. The depth and lateral extent of these hydrocarbon accumulation sites may improve seep emission models for the Coal Oil Point seep field.

1. Introduction

Marine hydrocarbon seeps (MHS) are pervasive across almost all continental margins and are an important part of the global carbon budget. Recent estimates indicate that these seeps account for up to a fifth of all global geological methane emissions (Etiope, 2009; Etiope et al., 2019). However, estimates of the total emissions from MHS have significant uncertainties as seeps can be irregularly active and the hydrocarbon migration pathways and shallow (<400 m) or near seabed accumulation of hydrocarbons are under-studied (Leifer, 2019). Many previously successful methods used to identify and estimate emission rates of MHS rely on the seep being active at the time of surveying. These methods have included side scan sonar, multibeam bathymetry, seismic profiling systems, gas capture systems, airborne spectroscopy, remote operated vehicles, and many others (e.g., Hornafius et al., 1999; Mitchell et al., 2018; Razaz et al., 2020; Leifer et al., 2006). Although these methods are useful for identifying seepage rates at the time of surveying, it has been noted in numerous studies that seep rates and seep areal extent can vary on subhourly, semidiurnal, diurnal, seasonal, and even on decadal scales (Leifer and Boles, 2005b; Fischer, 1975). Therefore, more information of the migration pathways and surrounding structures of MHS systems will aid in the understanding of overall seep activity.

A new method was developed to image hydrocarbon accumulation and migration related to MHS fields within the surrounding geology to a depth of 400 m below sea level. As hydrocarbons are significantly more electrically resistive than sediment, MHS systems are well-suited to detection by marine controlled-source electromagnetic (CSEM) methods (Constable, 2010; Constable and Srnka, 2007 & Orange et al., 2009). For the surveys presented here, a newly developed surface-towed CSEM system was deployed. This system is inexpensive and easy to use in a coastal setting (Sherman et al., 2017).

2. Study area

The Coal Oil Point (COP) MHS field is located offshore Isla Vista in Santa Barbara County, California, in water depths from a few meters to

* Corresponding author. Scripps Institution of Oceanography, University of California San Diego, La Jolla, CA, 92093, USA.
E-mail address: rbking@ucsd.edu (R.B. King).

https://doi.org/10.1016/j.marpetgeo.2022.105636
Received 25 October 2021; Received in revised form 4 March 2022; Accepted 7 March 2022
Available online 10 March 2022

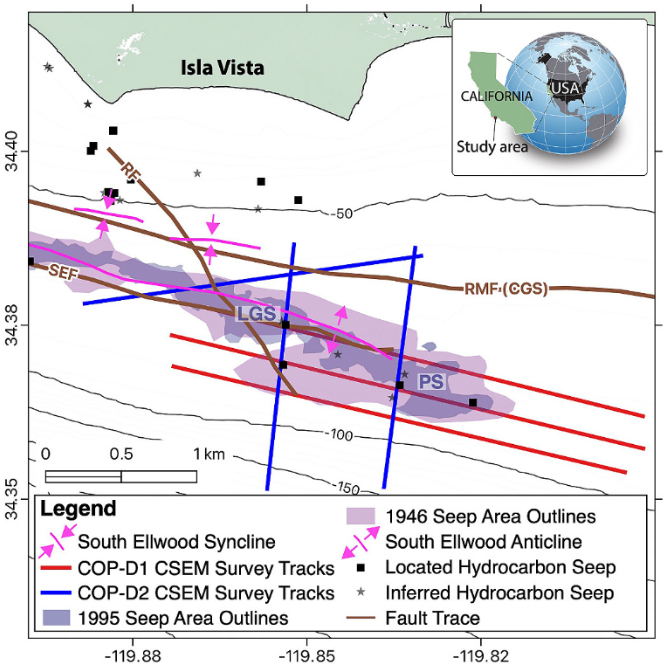

Fig. 1. Coal Oil Point seep field area offshore Isla Vista located within Santa Barbara County, California. COP-D1 CSEM Survey tracks (red lines) represent locations of data collected in January 2019. COP-D2 CSEM Survey tracks (blue lines) represent locations of data collected in May 2021. Survey track lines were chosen based on proximity to seep area outlined from 1995 seep gas spatial distributions by Hornafius et al. (1996) and inferred and located seep locations identified and defined by the USGS (Lorenson et al., 2009). The seep area outlined from 1946 gas and oil distributions is by Fischer (1978). La Goleta seep field is labeled LGS and Patch Seep is labeled PS (all seep names are informal). Finally, South Ellwood Anticline, South Ellwood Syncline, and fault locations from Leifer et al., (2010) and California Geological Survey are plotted: RF - Rudder Fault, RMF (CGS) - Red Mountain Fault trace by California Geological Survey (Treiman, 2006), SEF – South Ellwood Fault. Water depth contours are marked in black. (For interpretation of the references to color in this figure legend, the reader is referred to the Web version of this article.)

80 m (Fig. 1) and has two primary trends. The trend closer to the shoreline is in a few meters water depth and is associated with the folded and fractured source rock outcropping and seeping at the seabed. The offshore trend is in water depths of 50–100 m and is generally controlled by the South Ellwood Anticline. In this paper, the study area and the term COP are limited to the offshore seep area associated with the South Ellwood Anticline (see Fig. 1 for extent). Due to the prolific nature of this field and proximity to dense coastal populations, this area has been subject to numerous field investigations that have identified many seeps, geochemical markers, and the geologic structure underlying the region (e.g., Leifer, 2019; Lorenson et al., 2009; Hornafius et al., 1999; Kamerling et al., 2003). The stratigraphy of the COP seep field is folded, creating a series of structural traps for hydrocarbon accumulation within and above the source rock (Eichhubl et al., 2000). The source rock is capped by the relatively impermeable Sisquoc Formation and the traps are fed by fractures, faults, or through updip migration along bedding planes (Fig. 2) (Finkbeiner et al., 1997; Ogle et al., 1987).

Within the COP seep field, there are two main seep areas located along the South Ellwood anticline. The La Goleta MHS field is located near the shallowest crest of the Monterey Formation below the COP seep field and Patch Seep is located toward the eastern end of the COP seep field (Fig. 1). Based on the local geology, the accumulation site of the La Goleta MHS field and the Patch Seep should be located at least 1 km below sea level and controlled by the South Ellwood Anticline and South Ellwood Fault System (Leifer et al., 2010). La Goleta MHS field has displayed variable emission trends and hydraulic conductivity between different seeps (Bradley et al., 2010; Leifer, 2019) and delays have been observed between deep reservoir pressure changes and seepage rates (Leifer, 2019). These observations indicate that individual seeps may be connected at depth above the source rock. However, the locations of possible shared migration pathways or accumulation sites are not well defined.

The seep model for the COP MHS field described by Leifer and Boles (2005a) assumes a deep hydrocarbon reservoir plus an additional near-seabed reservoir to account for seepage behavior at La Goleta MHS field and Patch Seep. According to the model, seepage rates are pressure-sensitive and related to changes in hydrostatic pressure from tidal forcing and pressures from deep reservoirs. The balance of over-pressure and reservoir pressure result in changing emission rates at the seep sites (Leifer and Boles, 2005a; Leifer and Wilson, 2007). Generally,

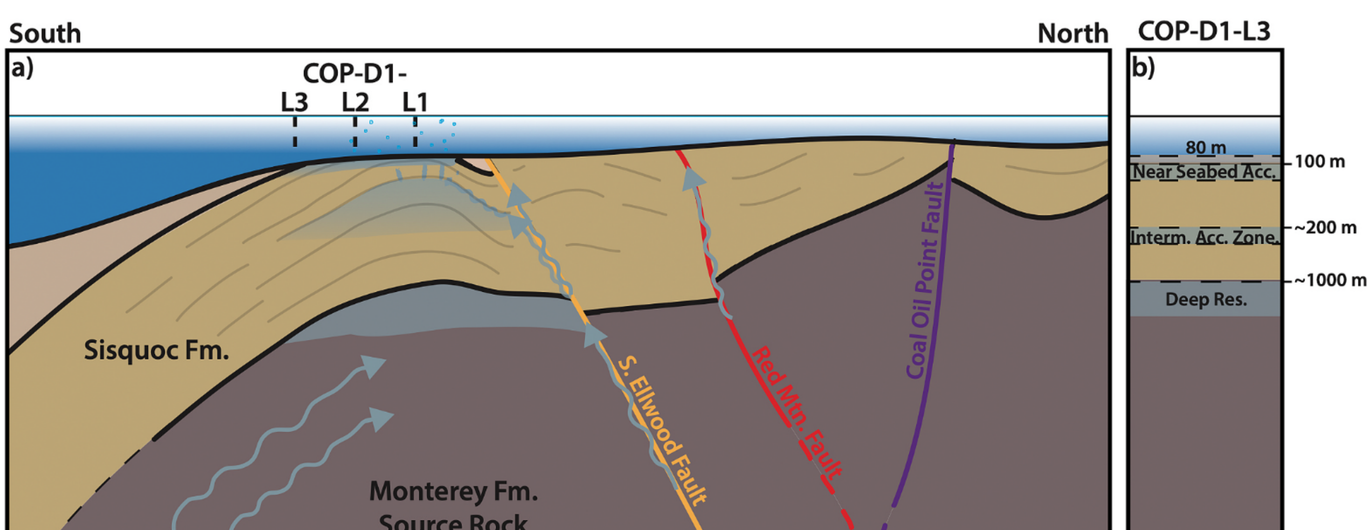

Fig. 2. a) Cartoon demonstrating potential fluid migration pathways (light blue arrows) upward from lower Monterey Formation (source rock) to intermediate near-seabed accumulation sites below the survey area. Illustration based on geologic models by Leifer et al., (2010). Note: illustration is not to scale. Dashed black lines indicate the intersection points of 2D resistivity profiles associated with the 2019 EM survey. b) illustrates hydrocarbon accumulation sites imaged in EM line COP-D1_L3 as well as a deep reservoir from previous studies (Leifer et al., 2010; Tennyson and Kropp, 1998). (For interpretation of the references to color in this figure legend, the reader is referred to the Web version of this article.)

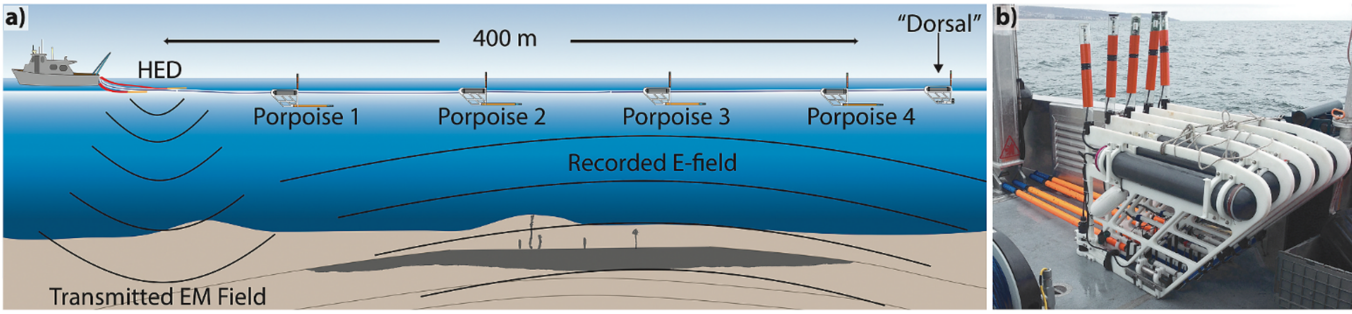

Fig. 3. a) Schematic of CSEM array used for survey offshore Isla Vista, Santa Barbara County, California. Horizontal electric dipole is labeled here as 'HED'. Here, the emitted electromagnetic field from the HED is labeled 'Transmitted EM Field'. b) Photo of all four porpoises (receivers) and dorsal (front) staged on deck. Logger is a grey pressurized case held in place with a white frame. GPS masts are orange vertical instruments affixed to the back of each white frame. The receiver frames have blue weights at the base to keep the instruments upright during towing operations. (For interpretation of the references to color in this figure legend, the reader is referred to the Web version of this article.)

the effect of hydrostatic pressure decreases with seabed depth (Boles et al., 2001). Leifer and Boles (2005b) predicted the lower bounds of tidal influencing through changing hydrostatic pressure in the COP region to be in water depths of 100–200 m. The flow of oil and gas from seep systems also is controlled by reservoir pressure, which increases with depth (Leifer and Wilson, 2007). The relationship between these two pressures is significantly impacted by the depth of the reservoir and the surrounding geology.

This marine CSEM study aimed to test the seep model of Leifer and Wilson (2007) by mapping the location of the hydrocarbon accumulation beneath La Goleta MHS field and Patch Seep. These fields are attractive targets to test for the existence of near-seabed hydrocarbon accumulation as upward hydrocarbon migration is controlled by the many local faults and the anticlinal structure could provide many potential intermediate traps for accumulation below the field.

3. Methodology

3.1. CSEM survey design

The marine CSEM method uses an electric current transmitter that emits electromagnetic fields that pass through seawater and propagate into the seafloor and to receivers, which measure the resulting electric fields, either on the seafloor or towed through the water. The recorded fields are proportional to electrical resistivity, making the method suitable for detecting hydrocarbons which are significantly more resistive in comparison to seawater or the surrounding seafloor sediment (e.g., Constable, 2010).

Because the water depths of La Goleta MHS field and Patch Seep are shallow, the custom-built small, low power, surface-towed CSEM system of Sherman et al. (2017) can be used effectively to map hydrocarbon occurrences to depths of 400 m below sea level. This system has the added benefit that it is inexpensive to use, can be hand-deployed, and requires a non-specialized vessel to efficiently survey the shelf. The system, illustrated in Fig. 3, consists of an electromagnetic transmitter, four electric field receivers, and a dorsal device that collects water-conductivity and water-depth data. The horizontal electric dipole, four receivers (referred to as porpoises), and dorsal are towed on the surface of the water on floating high molecular weight polyethylene rope, behind a vessel traveling between 2 and 4 knots. The frames of the receivers and dorsal are made from rigid plastic that is designed to slough off kelp or other ocean debris, to hold a rigid 2 m dipole 0.67 m beneath the sea surface, and to provide mounting for a vertical GPS mast that provides position and timing, and doubles as a flashing beacon for better visibility to other vessels. To maximize sensitivity to the predicted geology related to La Goleta MHS field, the receivers were separated by 100 m creating a maximum source-receiver spacing of 400 m and a total towed array length of 430 m. From sensitivity tests, the limits of sensitivity using this array are estimated to be at a depth between 400 and 500 m below sea level. Horizontal resolution is roughly 5–10% of the receiver to target distance; for example, if the investigation depth is 100 m below sea level, this array could yield horizontal resolution of 5–10 m at this depth.

The electromagnetic transmitter operates on 110–240 VAC power and outputs a GPS stabilized binary or ternary waveform. For this survey, the transmitter output was a 30-amp, current-controlled waveform-D of Meyer et al. (2011) on a 10-meter antenna. This configuration resulted in a 300 amp-meter horizontal electric dipole moment, a signal strength well suited to the source-receiver spacing chosen for this survey. Waveform-D was chosen as it generates higher amplitude responses in the 1st, 3rd, 7th, and 13th harmonics than other waveforms, allowing for collection of data across a broad frequency range (Meyer et al., 2011). The data presented here were collected during two separate cruises in January of 2019 and May of 2021. The survey design remained the same for both surveys except for the fundamental frequency of the waveform. A 2 Hz fundamental waveform was used to collect the initial 2019 CSEM data; following analysis of the data, the fundamental frequency was increased to 2.5 Hz for surveying in 2021 to increase the frequencies of the higher harmonics.

3.2. Survey data quality

A total of 37 km of high-quality inline electric field responses were collected in 350 min over the course of two survey days, one for each survey year (see Fig. 1 for survey locations). Following both surveys, the data were inspected for quality before processing. In January of 2019 (shown in red on Fig. 1), surveying from the FV Amigo, the last receiver in the array did not function because it reset, probably because of an impact that occurred during transportation, and the GPS mast of the first receiver in the array did not transmit data due to problems with a pin connection. In May of 2021 (shown in blue on Fig. 1), surveying from the RV Bob and Betty Beyster, the first receiver in the array malfunctioned due to a faulty battery. The rest of the receiver systems in both surveys functioned as designed.

3.3. Data processing and model design

Amplitude and phases of the CSEM response functions were extracted from the raw time-series data using a method detailed by Meyer et al. (2011). To increase the signal-to-noise ratio, the resulting transfer function estimates were stacked using an arithmetic mean to obtain the complex transfer function estimates for every stacking window along with an error estimate. Due to rough wave conditions (3 plus meter wave heights and 7 m/s wind gusts) in January 2019, stacking windows of 30 s were used. Sea state was calm in May of 2021 allowing for smaller stacking windows of 10 s to achieve similar errors to the previous survey

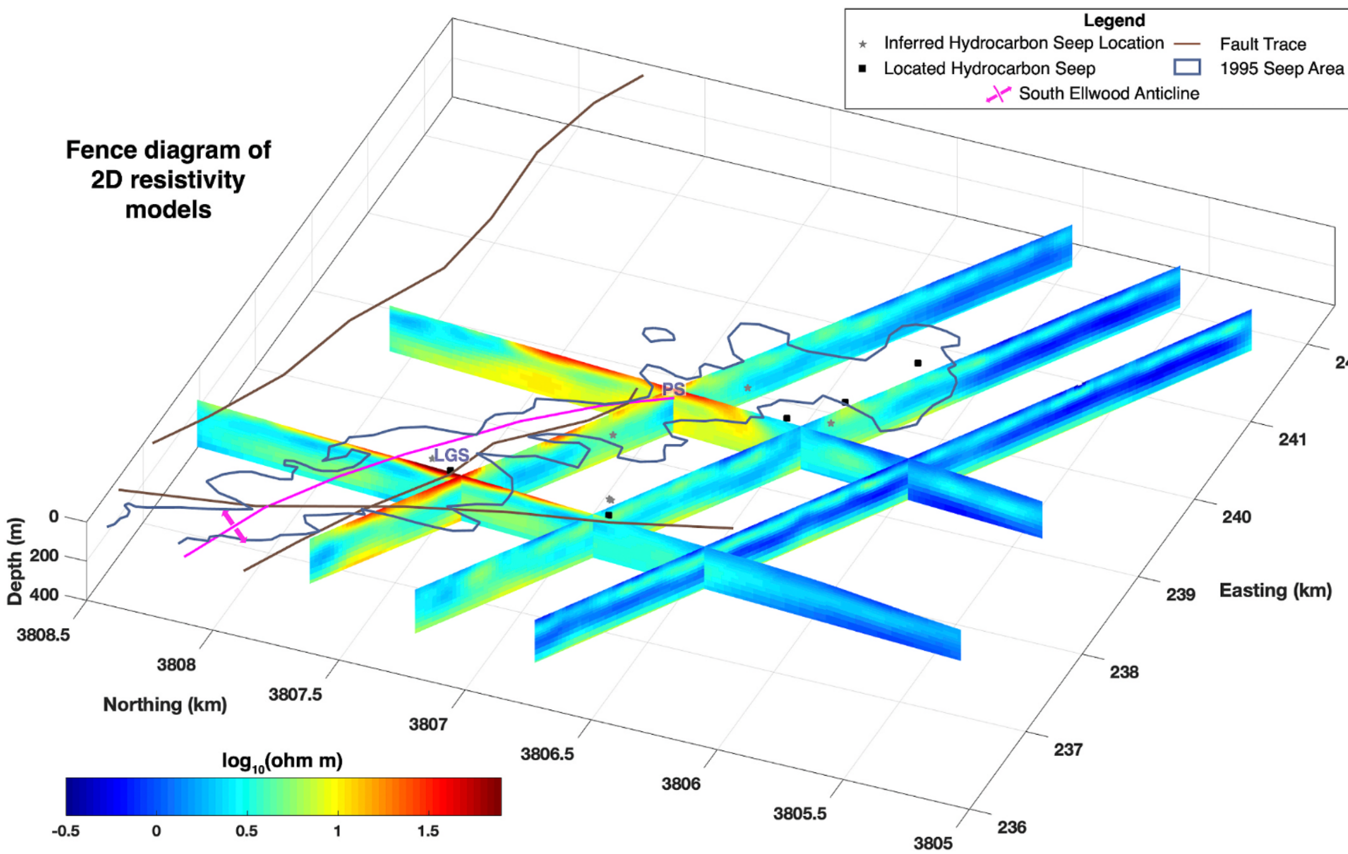

Fig. 4. Fence plot of 2D resistivity models over La Goleta MHS field (labeled here as 'LGS') and Patch Seep (labeled here as 'PS'); CSEM survey lines and dates of collection are also shown in Fig. 1. Dark blue lines indicate areal extent of seep gas distributions from Hornafius et al. (1996). Black squares indicate located seeps, and grey stars indicate the inferred location of seeps identified and defined by the USGS (Lorenson et al., 2009). Brown lines indicate the surface locations of the Rudder Fault, South Ellwood Fault (Leifer et al., 2010), and Red Mountain Fault (Treiman, 2006). Warm colors indicate high resistivity, inferred to be hydrocarbons. Coordinates in fence plot are UTM – Zone 11. (For interpretation of the references to color in this figure legend, the reader is referred to the Web version of this article.)

in 2019.

This method yielded high quality amplitude and phase response data for two receivers and three receivers as a function of position and frequency for the 2019 and 2020 surveys respectfully, although the first harmonic was excluded due to low signal to noise of the responses. The CSEM data associated with the 3rd, 7th, and 13th harmonics were well above the noise floor, making them suitable for inversion.

The modeling software used in this study is the publicly available, goal-oriented, adaptive, finite-element two-dimensional (2D) MARE2DEM inversion and modeling code of Key (2016). This code uses Occam's Inversion, a method that regularizes the inversion to obtain the smoothest resistivity model that fits the data (Constable et al., 1987). CSEM data were scrutinized manually for obvious outliers and subjected to a two-percent error floor for amplitude data and a one-percent error floor for phase data before being included in the model as finite-length dipoles. The 10 m-long horizontal electric dipole (HED) was modeled as a finite-length electric bipole and assumed to have a dip of 10°, consistent with direct observations during the survey.

The starting models included seawater as a fixed parameter, using conductivity data collected by the dorsal and available bathymetric data. Thus, the free inversion regions were reduced to the area below the seafloor and set to a uniform starting resistivity of 1 Ωm. Inversion parameter grids were constructed using quadrilateral cells that increased in height with depth to mimic the loss of resolution of the EM method with distance. Due to the adaptive nature of the MARE2DEM code, the computation grid was allowed to refine where necessary to accurately predict the model's data response (this is sometimes called the dual grid approach). The resistivity inversions were run to the minimum root mean square misfit possible; this value was then increased by ten percent to avoid overfitting and the final resistivity inversions converged to a root-mean-square misfit between 1 and 1.1, and are shown in Fig. 4.

4. Results and discussion

Below La Goleta MHS field and PS, the South Ellwood Anticline locally creates a trap in the fractured reservoir approximately 1 km below sea level (Fig. 2) (Leifer et al., 2010; Tennyson and Kropp, 1998). This reservoir is supplied by updip and near vertical hydrocarbon migration along thick damage zones (<20 m) associated with the South Ellwood Fault System (Leifer et al., 2010) from the deeper source rock (Kamerling et al., 2003). Further upward migration to shallow traps or to the seafloor is facilitated by the South Ellwood Fault System, Rudder Fault, other unmapped faults in the Monterey Formation, and open fractures and joints within the Sisquoc Formation.

The 2D resistivity models presented here contain several resistive anomalies below La Goleta MHS field, Patch Seep, and several unnamed seep sites (Fig. 4). The resistive anomalies collocated with known and inferred seep sites have resistivity values consistent with those expected from hydrocarbons (Constable, 2010), and so resistors encountered in this survey are interpreted to be hydrocarbons. Prior studies, based on water column and seafloor observations, have indicated that the areal extent of La Goleta MHS field is consistent and controlled by the South Ellwood Anticline and damage zones associated with the Rudder Fault (Washburn et al., 2005; Hornafius et al., 1999;Leifer et al., 2005a; Leifer, 2019). Conversely, the spatial extent of the Patch Seep has been

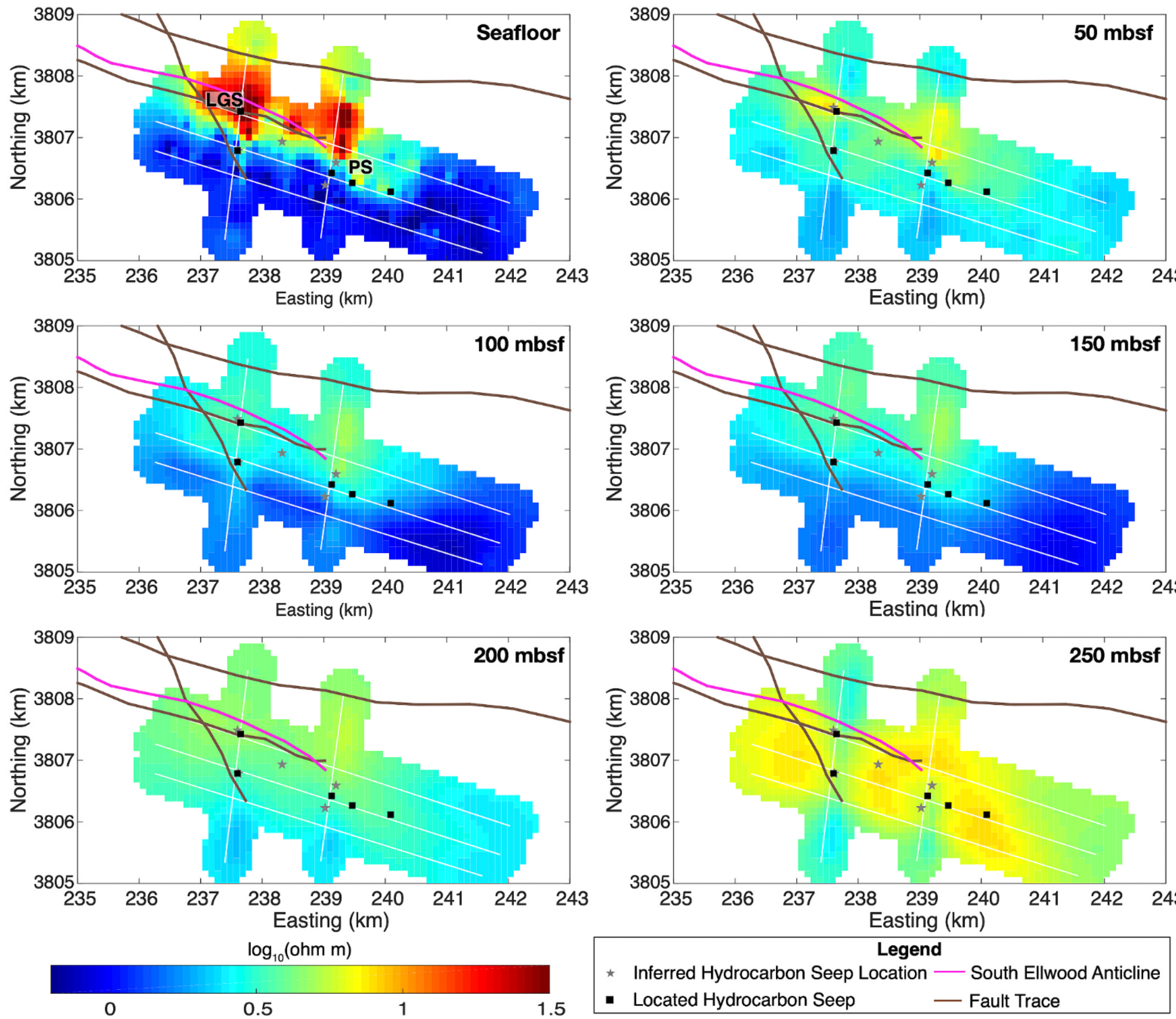

Fig. 5. Maps of logarithmic resistivity at and below the seafloor. Peak resistivity appears to correspond to the South Ellwood Anticline and is collocated with La Goleta MHS field, but is not collocated with Patch Seep. Peak resistivity is encountered both at the seafloor and again at approximately 250 m below seafloor (mbsf). The geometry of the seafloor and 250 mbsf resistor generally trend with the South Ellwood Anticline.

observed to change based on water column sampling studies; for example, the northern edge of the seep field has been recorded to shift up to ~600 m depending on the time of surveying (Fig. 1). The seafloor resistivity values modeled here are in agreement with these observations (Fig. 5). Previous maps of the La Goleta MHS field are collocated with high seafloor resistivity and vertical resistors below the seep field (Figs. 4, Fig. 5, and Fig. 6) (Hornafius et al., 1996; Fischer, 1978; Lorenson et al., 2009). These resistive features are collocated with the Rudder Fault, indicating hydrocarbon migration along related damage zones. Possibly due to changes in spatial extent of the Patch Seep, the highest seafloor resistivities near the Patch Seep are north of the area most recently mapped as an active seep site, although they are within previously mapped seep extents (Figs. 1 and 4). Additionally, a vertical resistor is imaged below Patch Seep which may be a hydrocarbon migration pathway within open fractures related to anticlinal flexure from the South Ellwood anticline (labeled in Fig. 6). There are several plausible reasons for the mismatch in seafloor resistivity and the most recent Patch Seep locations, most notably the presence of oily bubbles that can lead to oil deposition within the seep vents and bacterial or tar mats which can obstruct seepage, resulting in vent evolution or movement (Leifer, 2010).

Below the MHS presented here, a resistor approximately 25 m below the seafloor (mbsf) is pervasive across all survey lines (Fig. 4 and labeled 'near seabed reservoir' in Fig. 6). According to geologic models and seismic reflection profiles, this resistive layer is located within the Sisquoc Formation (Leifer et al., 2010; Kamerling et al., 2003; Sliter et al., 2008) and the feature could be produced from horizontal migration of hydrocarbons within a coarse layer of this formation (Fig. 2) (Boles et al., 2001; Boetius and Suess, 2004; Chen et al., 2021). This interpretation is supported by chip analysis from onshore and offshore wells that indicate local sandstone layers within the Sisquoc Formation (MacKinnon, 1989) and that the resistive layer appears to be constrained by the mapped anticline and synclines with several vertical features extending to known MHS locations. A trapping mechanism such as pore throat blockage or a change in permeability may lead to this near seafloor build-up of hydrocarbons. As this accumulation site is shallowly buried (~150 m total depth), changes in hydrostatic pressure through tidal forces may have a more pronounced effect on the associated MHS fields

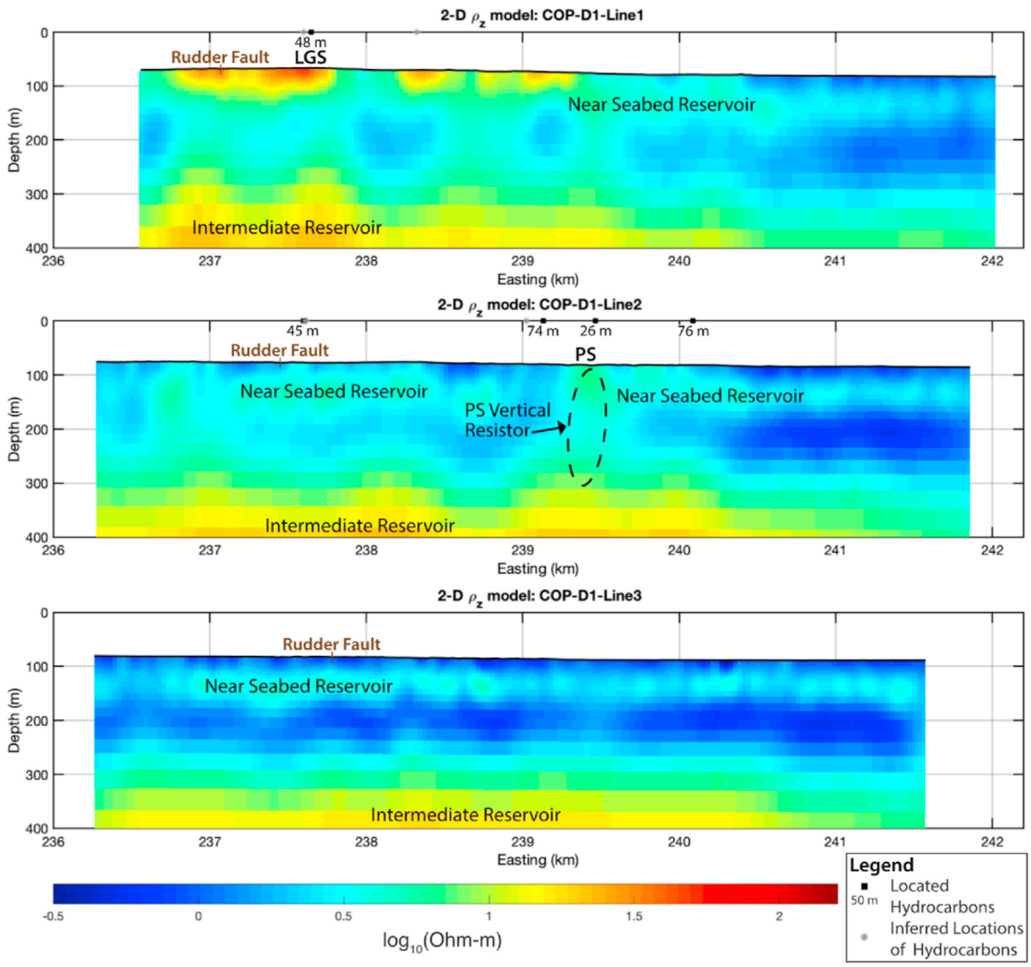

Fig. 6. 2D Resistivity Models of COP-D1 Lines 1 through 3 plotted with approximate locations of major seepage associated with La Goleta MHS Field (LGS) and Patch Seep (PD). Also plotted are locations of known and inferred seep locations as identified and defined by the USGS (Lorenson et al., 2009) with crossline distances to known hydrocarbon seep locations indicated. See Fig. 1 for plan view of model locations. The surface trace of the Rudder Fault is plotted in brown. Here, depth refers to meter below sea-level. (For interpretation of the references to color in this figure legend, the reader is referred to the Web version of this article.)

when compared to MHS fields supplied by deeper reservoirs.

Finally, a deeper resistor is encountered at approximately 200–250 mbsf within the Sisquoc Formation (Fig. 5 and labeled 'intermediate reservoir' in Fig. 6). This resistor appears to be constrained by the South Ellwood Anticline and has multiple vertical resistors connecting it to the seafloor seep locations (Fig. 6). Due to these observations, this resistor is interpreted as a hydrocarbon accumulation site that supplies the MHS fields above and the vertical features are interpreted to be migration pathways facilitated by open fractures related to the Rudder Fault or anticlinal flexure from the South Ellwood Anticline (Ogle et al., 1987). This accumulation zone is shallower than the previously identified hydrocarbon reservoirs located approximately 1000 m below La Goleta MHS Field. Therefore, the resistor located 200 to 250 mbsf could be an intermediate reservoir; a feature most recently proposed by Leifer (2019) to accurately model the temporal variability of seepage observed within COP. Before this CSEM survey, the existence of intermediate reservoirs beneath COP were inferred, but the depth and extent were not known.

5. Conclusion

The surface towed CSEM method used in this survey has been shown to be both efficient and effective at detecting marine hydrocarbon seep systems to total depths of 400 m. Our system detected two previously unidentified near seabed hydrocarbon accumulation sites which may supply the overlying MHS fields. The existence of one accumulation site is assumed in the model of Leifer (2019); however, the depth and lateral extent has not been characterized until now. The addition of this new knowledge in seep models could better constrain overall seep emission rates. Additionally, the 2D resistivity models indicate significant changes in extent and movement of the Patch Seep at the seafloor while the underlying MHS sources remain controlled by the South Ellwood Anticline. These results highlight the variability in the seafloor location of seeps and importance of studying the buried hydrocarbon accumulation sites and migration pathways to gain further insights into MHS character. More information is needed to characterize and predict the seep behavior in this region; however, CSEM methods could be useful in the identification of other hydrocarbon seep systems, as they can survey large regions relatively quickly and are sensitive to these targets.

Author contributions

Roslynn King: Conceptualization, Methodology, Investigation, Data curation, Writing – original draft, Visualization, Project administration **Steven Constable**: Validation, Resources, Writing - Reviewing and Editing **Jillian Maloney**: Writing - Reviewing and Editing, Funding acquisition, Supervision

Declaration of competing interest

The authors declare that they have no known competing financial interests or personal relationships that could have appeared to influence the work reported in this paper.

Acknowledgments

We thank the Captain and crew of the FV Amigo, Hannah Peterson, and Gregory Mamikunian who helped collect the 2019 data. We thank the Captain, Brett Pickering, of the RV Bob and Betty Beyster and Amy Gusick who helped collect the 2021 data. The authors are grateful for the technicians and engineers of the SIO EM Laboratory and support from the Scripps Seafloor Electromagnetic Methods Consortium. Additionally, we are very appreciative of the useful discussions with Amy Gusick from the Los Angeles Natural History Museum, Miriam Kastner from SIO, and Peter Kannberg from SIO. The ARCS Foundation generously supplements the PhD stipend of Roslynn King. Finally, we would like to thank the anonymous reviewer during the submission process for their thorough and insightful comments and suggestions. This work was supported by the National Center for Preservation Technology and Training – National Parks Service [P19AP00140, 2019].

References

Boetius, A., Suess, E., 2004. Hydrate Ridge: a natural laboratory for the study of microbial life fueled by methane from near-surface gas hydrates. Chem. Geol. 205, 291–310.
Boles, J.R., Clark, J.F., Leifer, I., Washburn, L., 2001. Temporal variation in natural methane seep rate due to tides, Coal Oil Point area, California. J. Geophys. Res.: Oceans 106 (C11), 27077–27086.
Bradley, E., Leifer, I., Roberts, D., 2010. Long-term monitoring of a marine geologic hydrocarbon source by a coastal air pollution station in Southern California. Atmos. Environ. 44 (38), 4973–4981.
Chen, C., Zheng, Z., Zeng, L.F., Xiao, F., Tian, L.P., Huang, K.Y., 2021. A combined geophysical and lithological study on eruptive history and Quaternary lacustrine stratigraphy of a maar in Leizhou Peninsula, China. J. Palaeogeogr. 10 (1), 1–14.
Constable, S., 2010. Ten years of marine CSEM for hydrocarbon exploration. Geophysics 75 (5), 75A67–75A81.
Constable, S.C., Parker, R.L., Constable, C.G., 1987. Occam's inversion: a practical algorithm for generating smooth models from electromagnetic sounding data. Geophysics 52 (3), 289–300.
Constable, S., Srnka, L.J., 2007. An introduction to marine controlled-source electromagnetic methods for hydrocarbon exploration. Geophysics 72 (2), WA3–WA12.
Eichhubl, P., Greene, H.G., Naehr, T., Maher, N., 2000. Structural control of fluid flow: offshore fluid seepage in the Santa Barbara Basin, California. J. Geochem. Explor. 69, 545–549. https://doi.org/10.1016/S0375-6742(00)00107-2.
Etiope, G., 2009. Natural emissions of methane from geological seepage in Europe. Atmos. Environ. 43 (7), 1430–1443.
Etiope, G., Schwietzke, S., Helmig, D., Palmer, P., 2019. Global geological methane emissions: an update of top-down and bottom-up estimates. Elementa: Science of the Anthropocene 7.
Finkbeiner, T., Barton, C.A., Zoback, M.D., 1997. Relationships among in-situ stress, fractures and faults, and fluid flow: Monterey Formation, Santa Maria Basin, California. AAPG Bull. 81 (12), 1975–1999.
Fischer, P.J., 1975. Natural Gas and Oil Seeps, Santa Barbara Basin. California State University, Department of Geosciences, California.
Fischer, P.J., 1978. Oil and tar seeps, Santa Barbara basin, California. In: Everitts, D.J., Paul, R.G., Eaton, C.F., Welday, E.E. (Eds.), California Offshore Gas, Oil and Tar Seeps. California State Lands Commission, Sacramento, California, pp. 1–62.
Hornafius, J.S., Luyendyk, B.P., Kamerling, M.J., 1996. Seismic Mapping of the North Channel Fault Near Santa Barbara, California, vol. 2. Annual Rep Southern California Earthquake Center, pp. D13–D17, 1995.
Hornafius, J.S., Quigley, D., Luyendyk, B.P., 1999. The world's most spectacular marine hydrocarbon seeps (Coal Oil Point, Santa Barbara Channel, California): quantification of emissions. J. Geophys. Res. 104 (C9), 20703–20711. https://doi.org/10.1029/1999JC900148.
Kamerling, M., Horner, S., Thompson, L., 2003. The Monterey Formation at South Ellwood field, Santa Barbara channel, California. In: Proceedings Society of Petroleum Engineers Western Regional/AAPG Pacific Section Joint Meeting, Long Beach. California, Bakersfield, CA, USA. May.
Key, K., 2016. MARE2DEM: a 2-D inversion code for controlled-source electromagnetic and magnetotelluric data. Geophys. J. Int. 207 (1), 571–588.
Leifer, I., 2010. Characteristics and scaling of bubble plumes from marine hydrocarbon seepage in the Coal Oil Point seep field. J. Geophys. Res.: Oceans 115 (C11).
Leifer, I., 2019. A Synthesis Review of Emissions and Fates for the Coal Oil Point Marine Hydrocarbon Seep Field and California Marine Seepage. Geofluids, 2019.
Leifer, I., Boles, J., 2005a. Measurement of marine hydrocarbon seep flow through fractured rock and unconsolidated sediment. Mar. Petrol. Geol. 22 (4), 551–568.
Leifer, I., Boles, J., 2005b. Turbine tent measurements of marine hydrocarbon seeps on subhourly timescales. J. Geophys. Res.: Oceans 110 (C1).
Leifer, I., Kamerling, M.J., Luyendyk, B.P., Wilson, D.S., 2010. Geologic control of natural marine hydrocarbon seep emissions, Coal Oil Point seep field, California. Geo Mar. Lett. 30, 331–338, 3–4.
Leifer, I., Roberts, D., Margolis, J., Kinnaman, F., 2006. In situ sensing of methane emissions from natural marine hydrocarbon seeps: a potential remote sensing technology. Earth Planet Sci. Lett. 245, 509–522, 3–4.
Leifer, I., Wilson, K., 2007. The tidal influence on oil and gas emissions from an abandoned oil well: nearshore Summerland, California. Mar. Pollut. Bull. 54 (9), 1495–1506.
Lorenson, T.D., Hostettler, F.D., Rosenbauer, R.J., Peters, K.E., Dougherty, J.A., Kvenvolden, K.A., Gutmacher, C.E., Wong, F.L., Normark, W.R., 2009. Natural Offshore Oil Seepage and Related Tarball Accumulation on the California Coastline – Santa Barbara Channel and the Southern Santa Maria Basin; Source Identification and Inventory, p. 116. USGS Open-File Report 2009-1225.
MacKinnon, T.C., 1989. Petroleum geology of the Monterey Formation in the Santa maria and Santa Barbara coastal and offshore areas. Oil in the California Monterey Formation: Field Trip Guide Bk. 311, 11–27.
Mitchell, G.A., Orange, D.L., Gharib, J.J., Kennedy, P., 2018. Improved detection and mapping of deepwater hydrocarbon seeps: optimizing multibeam echosounder seafloor backscatter acquisition and processing techniques. Mar. Geophys. Res. 39, 323–347, 1–2.
Meyer, D., Constable, S., Key, K., 2011. Broad-band waveforms and robust processing for marine CSEM surveys. Geophys. J. Int. 184 (2), 689–698. https://doi.org/10.1111/j.1365-246X.2010.04887.x.
Ogle, B.A., Wallis, W.S., Heck, R.G., Edwards, E.B., 1987. Petroleum Geology of the Monterey Formation in the Offshore Santa Maria/Santa Barbara Areas. Prentice-Hall, Englewood Cliffs, New Jersey, pp. 382–406.
Orange, A., Key, K., Constable, S., 2009. The feasibility of reservoir monitoring using time-lapse marine CSEM. Geophysics 74 (2).
Razaz, M., Di Iorio, D., Wang, B., Asl, S.D., Thurnherr, A.M., 2020. Variability of a natural hydrocarbon seep and its connection to the ocean surface. Sci. Rep. 10 (1), 1–13.
Sherman, D., Kannberg, P., Constable, S., 2017. Surface towed electromagnetic system for mapping of subsea Arctic permafrost. Earth Planet Sci. Lett. 460, 97–104.
Sliter, R.W., Triezenberg, P.J., Hart, P.E., 2008. High-Resolution Chirp and Mini-Sparker Seismic-Reflection Data from the Southern California Continental Shelf–Gaviota to Mugu Canyon.
Tennyson, M.E., Kropp, A.P., 1998. Regional cross section across Santa Barbara channel from northwestern Santa rosa island to Canada de Molino. In: Kunitomi, D.S., Hopps, T.E., Galloway, J.M. (Eds.), Structure and Petroleum Geology, Santa Barbara Channel, California, Miscellaneous Publication 46. Pacific Section AAPG, Bakersfiled, CA, pp. 185–193.
Treiman, J.A., 2006. Fault number 90, Red Mountain fault zone in Quaternary fault and fold database of the United States. US Geol. Survey Available at. https://earthquakes.usgs.gov/hazards/qfaults.
Washburn, L., Clark, J.F., Kyriakidis, P., 2005. The spatial scales, distribution, and intensity of natural marine hydrocarbon seeps near Coal Oil Point, California. Mar. Petrol. Geol. 22 (4), 569–578.